

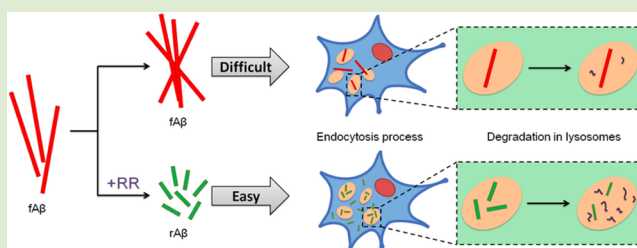
In Vitro Studies on Accelerating the Degradation and Clearance of Amyloid- β Fibrils by an Antiamyloidogenic Peptide

Qian Zhang,[†] Jing Liu,[†] Xiaoyu Hu, Wei Wang,* and Zhi Yuan*

Key Laboratory of Functional Polymer Materials of Ministry of Education, Institute of Polymer Chemistry, Collaborative Innovation Center of Chemical Science and Engineering (Tianjin), Nankai University, Tianjin 300071, China

Supporting Information

ABSTRACT: The clearance of overloaded amyloid- β ($A\beta$) species, especially the toxic aggregates, was thought to be an attractive and promising strategy for Alzheimer's disease (AD) therapy in the past decade. In this work, an active $A\beta$ inhibitor decapeptide RR was used to transform mature $A\beta$ fibrils ($fA\beta$) into nanorod-like $A\beta$ assemblies ($rA\beta$) as well as loosen the β -structure of $rA\beta$. Compared with $fA\beta$, $rA\beta$ could be engulfed by PC12 cells more efficiently and showed a 1.46-fold difference. More importantly, the $rA\beta$ was colocalized with lysosomes after endocytosis, and in vitro study illustrated that $rA\beta$ were easily degraded by lysosome protease cathepsin B when compared with the fibrils. Thus, our study indicated the potential application of RR in $A\beta$ fibrils clearance by a cell-participated and enzyme-mediated pathway.



Alzheimer's disease (AD), as a neurodegenerative disorder, is the most common form of dementia in humans. It is widely accepted that the process of amyloid- β peptides ($A\beta$) self-assembly into soluble oligomers, protofibrils, and finally insoluble mature fibrils with β -sheet structure is the significant step inducing AD. Since the soluble oligomer is the most toxic species,^{1–4} many studies have focused on designing various inhibitors, such as small molecules binding with hydrophobic core of $A\beta$ ⁵ or chelating agents targeting metal- $A\beta$ species,^{6–8} against $A\beta$ aggregation and reduce its cytotoxicity successively. However, recent research also suggests that the insufficient clearance rather than the excessive production of $A\beta$ contributes more to its accumulation.^{9,10} Therefore, the clearance of overloaded $A\beta$, especially those with the β -sheet structure, becomes a potential therapeutic strategy for AD.

Cellular engulfment is an important mechanism for clearing the toxic protein in the brain, and once the toxic protein is internalized, it can be degraded by various proteases. Thus, during the past decade, cell-participated and enzyme-mediated degradation of $A\beta$ has attracted a huge amount of attention.^{11–13} Xiao et al. found that the transcription factor EB could stimulate the internalization and in turn the degradation of $A\beta$ via lysosomes.¹³ It has been also reported that $A\beta$ fibrils ($fA\beta$), via the process of receptor-mediated cell uptake, could be transported within the endosomal-lysosomal pathway and then degraded by proteases such as cathepsin B and D in lysosomes.^{14,15} However, due to its big size and intermolecular parallel β -sheets structure, $fA\beta$ exhibits relatively lower cellular uptake efficiency and degradation rate than other types of $A\beta$.^{16–18} Consequently, decreasing the size and β -sheets content in aggregates would benefited for increasing the uptake of $fA\beta$ and promoting its degradation in lysosome.

In our previous work, an active decapeptide inhibitor RR (RYAAFFARR) was designed, which enables 75% inhibition of $A\beta_{40}$ fibrillation at an equimolar concentration and a complete inhibition at a molar ratio of 1:4 ($A\beta$ /RR).¹⁹ Herein, we found that RR could also transform the $A\beta$ mature fibril into nanorod-like fragments ($rA\beta$), which is also a less toxic form of $A\beta$ according to our following study. To our knowledge, the rod-like nanoparticles could be easily internalized by the endocytosis and show a more rapid cell uptake rate.^{20,21} Therefore, we suppose that compared with $fA\beta$, $rA\beta$ could be easier endocytosed by cells into lysosome and in turn degraded by lysosomal enzymes.

To investigate the transformation effect of RR on $fA\beta$, thioflavin-T (ThT) fluorescence assay was first used. As shown in Figure 1a, the fluorescence intensity kept increasing with the incubation of $A\beta$ monomer solution in the first day, then it remained stable in the next 2 days, illustrating that the fibrils were generated. This result was supported by TEM (Figure 1b), consistent with our previous work.¹⁹ After RR added in the fibrils solution, the fluorescence intensity decreased quickly in the first day, indicating the destruction of β -sheet structure. When the curve became stable after 2 days coinubation, the ThT fluorescence intensity of $A\beta$ fibrils decreased about 45% both with a molar ratio of 1:1 and 1:5 ($A\beta$ /RR). Since the reduction of fluorescence intensity may result from the competitive binding between RR and ThT toward the fibrils, circular dichroism (CD) was used for confirming it. Fortunately, the decrease of β -sheet structure in $fA\beta$ after

Received: January 15, 2015

Accepted: March 6, 2015

Published: March 9, 2015

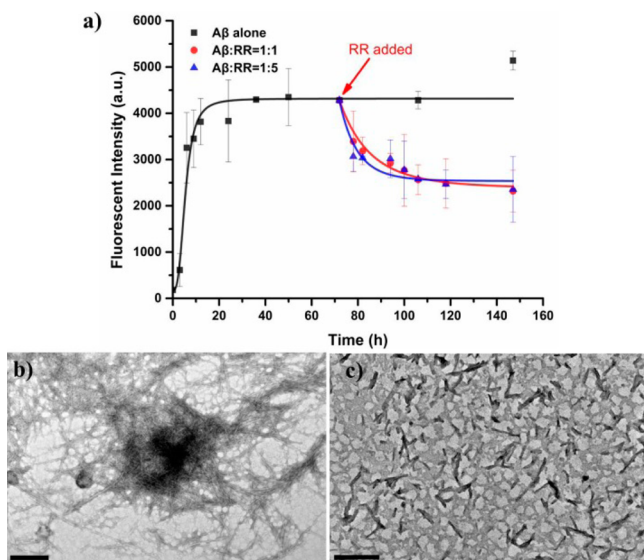


Figure 1. (a) Monitoring detection of $A\beta$ fibrillation and transformation by RR using a ThT fluorescence assay. The fibrils were incubated with $20 \mu\text{M}$ $A\beta$ monomer, and then RR was dissolved in $A\beta$ fibril solution with a molar ratio of 1:1 and 1:5, respectively ($n = 3$). (b, c) Negative-staining TEM images of $fA\beta$ and $rA\beta_{1:1}$ after 3 days incubation. Scale bars = 500 nm.

treated with RR was also observed by CD spectrum (Figure S1). TEM images were easy to see that the mature fibrils (Figure 1b) with a length of $1 \mu\text{m}$ or more, actually transformed into nanorod-like fragments (200–250 nm), after eliminating the possibility of the self-assembling of RR (Figure S2). In addition, the obtained $rA\beta$ treated with RR of 1:1 (Figure 1c) and 1:5 (Figure S3) molar ratio (represented by $rA\beta_{1:1}$ and $rA\beta_{1:5}$, respectively) had a similar morphology. Because of the great reduction in length, $rA\beta$ may be easier for cellular uptake, and the reduction of β -sheet structure may make it facilitated for enzyme-mediated degradation.^{16,17} The transformation effect of $A\beta$ inhibitor on $A\beta$ fibril was also reported by other researchers. Chafekar et al. reported a four KLVFF peptides modified dendrimer (K4) and found that K4 could lead to the disassembly of existing aggregates.²² Although lacking the direct evidence, most studies are apt to attribute this event to the competitive binding between the inhibitor and $A\beta$ fibril.

It is notable that the width of these $rA\beta$ was about 25 nm (Figures 1c and S3), which was greater than $A\beta$ protofibril ($\sim 5 \text{ nm}$)^{23,24} and $A\beta$ mature fibrils ($\sim 13\text{--}20 \text{ nm}$).^{25,26} Thus, we tend to suppose that the RR not only broke the fibrils into fragments, but also bind with $rA\beta$. Moreover, in electrophoresis and MALDI-TOF mass assay, we did not find the corresponding band or molecular ion peak of $A\beta$ oligomers (data not shown here). All these results indicated that instead of completely transforming the $fA\beta$ into protofibrils or soluble oligomers, RR partly broke the fibrils into nanorod-like fragments.

Recent research has illustrated that $A\beta$ monomers, oligomers, and protofibrils can interconvert and keep a balance.²⁷ Once protofibrils grow into fibrils, the latter are insoluble and cannot easily be disassembled.²⁸ Compared with $A\beta$ monomer and mature fibrils, oligomers and protofibrils are much more neurotoxic.^{29–31} Based on these facts, MTT assay was used to examine the cytotoxicity of $rA\beta$ on neuronal PC12 cells.³² $A\beta$ monomers, fibrils, and transformation solutions with the same

concentration were added to the cells respectively and cell viability was determined after 48 h. The results (Figure 2)

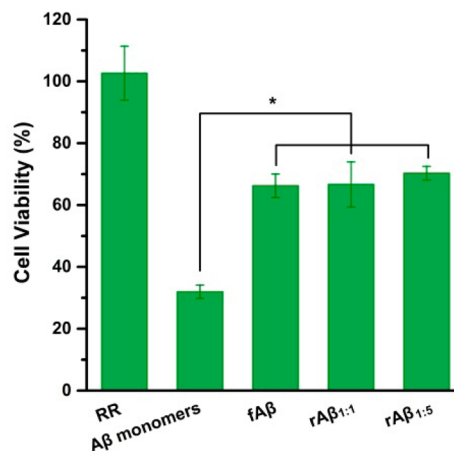


Figure 2. Cytotoxicity of RR and different $A\beta$ species to PC12 cells. The concentration of all samples was $20 \mu\text{M}$. $A\beta$ fibrils, $rA\beta_{1:1}$ and $rA\beta_{1:5}$ had a great improvement in cell viability compared with $A\beta$ monomer and they had no significant difference with each other. Cell viability was determined using MTT assay ($n = 5$). Statistical significance level is expressed by asterisks: $*p < 0.01$.

demonstrated that $rA\beta$ was much less potent to induce cytotoxicity than $A\beta$ monomer. And the similar toxicity of $rA\beta$ and $fA\beta$ indicated the structural homologue of them. It is also corresponding with our pervious hypothesis.

To further investigate whether the transformation of $fA\beta$ could facilitate its cellular uptake, $fA\beta$ and $rA\beta$ were labeled by FITC, and flow cytometry (FCM) was used to detect the internalized quantity of $A\beta$ assemblies by PC12 cells. FITC-labeled $fA\beta$ and $rA\beta$, at a concentration of $2 \mu\text{M}$, was cocultured with PC12 cells from 1 to 24 h. The total fluorescence intensity (TFI) of both fibrils and fragments increased significantly during the first 6 h, demonstrating the cellular uptake of $rA\beta$ and $fA\beta$. After treated with the $A\beta$ assemblies for 9 h, the TFI of $rA\beta$ and $fA\beta$ in the cellular fraction decreased, and the TFI in PC12 treated with $fA\beta$, $rA\beta_{1:1}$, and $rA\beta_{1:5}$ showed a similar variation tendency (Figures 3a and S4). Therefore, we chose the maximum TFI point (6 h) to examine the effect of transformation on the cellular uptake

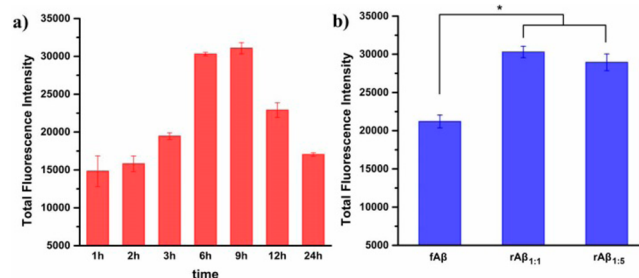


Figure 3. Cellular uptakes of $fA\beta$, $rA\beta_{1:1}$, and $rA\beta_{1:5}$ in PC12 cells. The concentrations of all samples were $2 \mu\text{M}$. (a) Total fluorescence intensity of FITC-labeled $rA\beta_{1:1}$ after incubation for 1, 2, 3, 6, 9, 12, and 24 h, respectively. (b) Total fluorescence intensity of FITC-labeled $fA\beta$, $rA\beta_{1:1}$, and $rA\beta_{1:5}$ in cells measured by FCM after incubation for 9 h. Data points shown are the mean values \pm SD from three independent experiments. Statistical significance level is expressed by asterisks: $*p < 0.01$.

(Figure 3b). As we expected, the cellular uptake of $rA\beta_{1:1}$ was approximately 1.46 times higher than $fA\beta$ ($p < 0.01$), suggesting that the great decrease in size may facilitate cellular internalization. And due to the similar particle shape and size, $rA\beta_{1:1}$ and $rA\beta_{1:5}$ did not show a statistical significant difference.

The decrease of $A\beta$ assemblies in PC12 cells perhaps attributed to two reasons: degradation in lysosome or exocytosis by the cells. So confocal microscopy was used to test the intracellular distribution of $rA\beta$ and $fA\beta$ in cells, and trail the fate after their internalization. PC12 cells were exposed to FITC-labeled $rA\beta$ for 3 h and LysoTracker Red was used to visualize lysosomes. It could be seen in Figure 4 that the green

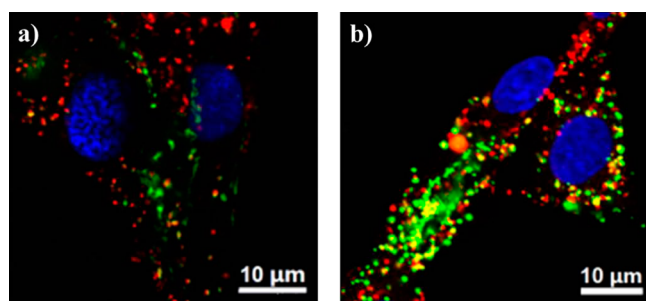


Figure 4. CLSM images of FITC-labeled (a) $fA\beta$ and (b) $rA\beta_{1:1}$ (green) with a concentration of $2 \mu\text{M}$ in PC12 cells after incubation for 3 h. Lysosome (red) was indicated by LysoTracker Red. Cell nuclei (blue) were labeled with DAPI. There was more $rA\beta_{1:1}$ in cells and $rA\beta_{1:1}$ was colocalized with the signal of LysoTracker (yellow) compared with $fA\beta$. Scale bars = $10 \mu\text{m}$.

fluorescence in the cell culture with $rA\beta$ was obviously stronger than that of $fA\beta$, consistent with the previous FCM result. What's more, we could find lots of colocalization areas (yellow) of $rA\beta$ (green) and lysosome (red) in Figure 4b, indicating $rA\beta$ was colocalized in lysosomes and possible to be degraded in PC12 cells. This phenomenon could not be obviously observed in $fA\beta$ -treated cells, and that maybe because the small quantity of $fA\beta$ in cells or the possible exocytosis by cells to clear it.¹⁷

According to previous research, $A\beta$ is degraded by a large set of proteases with diverse characteristics.³³ Among them, cathepsin B (CatB), a cysteine protease of the papain superfamily, degrades peptides and proteins that enter the endosome/lysosomal system by endocytosis or phagocytosis.³⁴ It is associated with amyloid plaques in AD brains³³ and it can effectively cleave $A\beta_{42}$, generating C-terminally truncated $A\beta$ peptides that are less amyloidogenic under cell-free condition.³⁵ Thus, CatB was chosen to carry out our in vitro degradation of $rA\beta$ and $fA\beta$ in the following experiments to explore the possibility of the degradation of $rA\beta$ after cellular uptake.

After incubating CatB and $A\beta$ monomer/assemblies for 2 h, $A\beta$ were proteolytic cleaved into diverse segments by CatB, which was detected by MALDI-TOF mass spectrometry, and the degraded segments of $rA\beta$ were corresponding with those of $A\beta$ monomer and $fA\beta$ (Figure 5). From the degradation products of $A\beta$ monomer, it could be seen that CatB has a high activity at Lys₁₆-Leu₁₇, Leu₁₇-Val₁₈, Gly₃₃-Leu₃₄, and Val₃₆-Gly₃₇. It is a favorable property, since $A\beta_{16-20}$ and $A\beta_{31-40}$ are the major hydrophobic regions for the aggregation of $A\beta$,³⁶ these C-terminally truncated peptides ($A\beta_{1-36}$, $A\beta_{1-33}$, $A\beta_{1-17}$, and $A\beta_{1-16}$) will show less fibrillogenic capacity than full-length $A\beta_{40}$. What's more, the degradation products of $rA\beta$ have a relative higher quantity of $A\beta_{40}$, and there are more C-

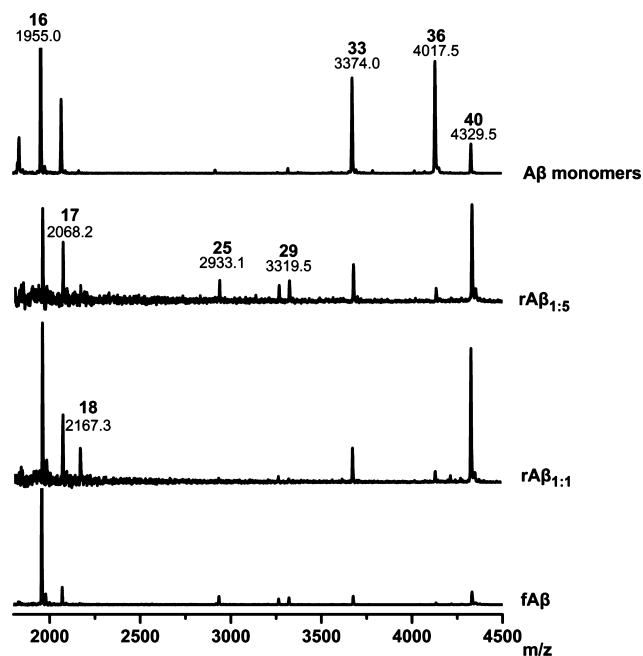


Figure 5. MALDI-TOF mass spectrometry of the cleavage of fresh $A\beta$ monomer, $fA\beta$, $rA\beta_{1:1}$, and $rA\beta_{1:5}$ by pure CatB ($0.5 \mu\text{g/mL}$) at pH 6.0 (25 mM MES buffer) for 2 h.

terminally truncated peptides in the degradation products of $rA\beta_{1:5}$ than that of $rA\beta_{1:1}$. We suppose this may because of the looser structure of $rA\beta$ than $fA\beta$'s. This less compact structure of $rA\beta$ (especially $rA\beta_{1:5}$) made it easier for the cleavage of CatB, and even made it possible for CatB disaggregating the monomers from $rA\beta$. In addition, the degradation products of $fA\beta$ were more difficultly detected than monomers and $rA\beta$ s, suggesting that the compact intermolecular parallel β -sheets structure of $fA\beta$ made the most cleavage-active sites inaccessible to enzymolysis. One exception is that the quantity of $A\beta_{1-16}$ segments seemed higher than other peaks in the degradation products of $fA\beta$. This may come from the cleavage directly from the fibrils, since $A\beta_{1-16}$ is near to the N-terminal of $A\beta$, which have a random-coil structure. Once an $A\beta$ molecule in fibrils was cleaved at Lys₁₆-Leu₁₇, the $A\beta_{1-16}$ segment was easier to separate and the $A\beta_{17-40}$ segment might remain in the fibril. Altogether, the fact that $rA\beta$ were highly susceptible to degrade as compared with fibrils (Figure 5), suggests the promising ability of RR to transform $fA\beta$ and facilitate $A\beta$ fibrils degradation in lysosome after cellular internalization.

In summary, an anti-amyloidogenic peptide RR was used to transform the mature $A\beta$ fibril into 250-nanometers-long nanorod-like fragments. These fragments were less cytotoxic than amyloidogenic $A\beta$ intermediates and the variance in shape greatly facilitated their cellular internalization. Their colocalization with lysosome after endocytosis and degradation by lysosomal enzyme in vitro greatly indicated the possibility of successfully clearing $rA\beta$ in a cell-participated and enzyme-mediated pathway. Thus, our research findings provided a potential method to decrease the accumulation of $A\beta$ from its fibril formation. Further structural studies at high resolution, such as NMR and docking calculations,^{37,38} are still needed to fully understand the role of RR in this transformation process. Altogether, these results, integrated with our previous work,¹⁹ indicated that the decapeptide RR could both inhibit the

aggregations of A β and disaggregate the mature A β fibril, which makes it a promising modulating molecule for AD treatment.

■ ASSOCIATED CONTENT

■ Supporting Information

Experimental details and supplementary data. This material is available free of charge via the Internet at <http://pubs.acs.org>.

■ AUTHOR INFORMATION

Corresponding Authors

*E-mail: duroo@nankai.edu.cn.

*E-mail: zhiy@nankai.edu.cn.

Author Contributions

[†]These authors contributed equally to this work (Q.Z. and J.L.).

Notes

The authors declare no competing financial interest.

■ ACKNOWLEDGMENTS

This work was supported by National Natural Science Foundation of China (51273094) and PCSIRT (IRT1257). We also thank Professor Hua Tang, Tianjin Medical University, for his technical suggestion on cell-related experiments.

■ REFERENCES

- (1) Kotler, S. A.; Walsh, P.; Brender, J. R.; Ramamoorthy, A. *Chem. Soc. Rev.* **2014**, *43*, 6692.
- (2) Sciacca, M. F.; Kotler, S. A.; Brender, J. R.; Chen, J.; Lee, D.-k.; Ramamoorthy, A. *Biophys. J.* **2012**, *103*, 702.
- (3) Brender, J. R.; Salamekh, S.; Ramamoorthy, A. *Acc. Chem. Res.* **2011**, *45*, 454.
- (4) Vivekanandan, S.; Brender, J. R.; Lee, S. Y.; Ramamoorthy, A. *Biochem. Biophys. Res. Commun.* **2011**, *411*, 312.
- (5) Sinha, S.; Lopes, D. H. J.; Du, Z.; Pang, E. S.; Shanmugam, A.; Lomakin, A.; Talbiersky, P.; Tennstaedt, A.; McDaniel, K.; Bakshi, R.; Kuo, P. Y.; Ehrmann, M.; Benedek, G. B.; Loo, J. A.; Klärner, F. G.; Schrader, T.; Wang, C.; Bitan, G. *J. Am. Chem. Soc.* **2011**, *133*, 16958.
- (6) Choi, J.-S.; Braymer, J. J.; Nanga, R. P.; Ramamoorthy, A.; Lim, M. H. *Proc. Natl. Acad. Sci. U.S.A.* **2010**, *107*, 21990.
- (7) DeToma, A. S.; Salamekh, S.; Ramamoorthy, A.; Lim, M. H. *Chem. Soc. Rev.* **2012**, *41*, 608.
- (8) Ramamoorthy, A.; Lim, M. H. *Biophys. J.* **2013**, *105*, 287.
- (9) Bateman, R. J.; Munsell, L. Y.; Morris, J. C.; Swam, R.; Yarasheski, K. E.; Holtzman, D. M. *Nat. Med.* **2006**, *12*, 856.
- (10) Mawuenyega, K. G.; Sigurdson, W.; Ovod, V.; Munsell, L.; Kasten, T.; Morris, J. C.; Yarasheski, K. E.; Bateman, R. J. *Science* **2010**, *330*, 1774.
- (11) Miners, J. S.; Baig, S.; Palmer, J.; Palmer, L. E.; Kehoe, P. G.; Love, S. *Brain Pathol.* **2008**, *18*, 240.
- (12) Li, W.; Tang, Y.; Fan, Z.; Meng, Y.; Yang, G.; Luo, J.; Ke, Z.-J. *Mol. Neurodegener.* **2013**, *8*, 27.
- (13) Xiao, Q.; Yan, P.; Ma, X.; Liu, H.; Perez, R.; Zhu, A.; Gonzales, E.; Burchett, J. M.; Schuler, D. R.; Cirrito, J. R. *J. Neurosci.* **2014**, *34*, 9607.
- (14) Chung, H.; Brazil, M. I.; Soe, T. T.; Maxfield, F. R. *J. Biol. Chem.* **1999**, *274*, 32301.
- (15) Koenigsnecht, J.; Landreth, G. J. *Neurosci.* **2004**, *24*, 9838.
- (16) Crouch, P. J.; Tew, D. J.; Du, T.; Nguyen, D. N.; Caragounis, A.; Filiz, G.; Blake, R. E.; Trounce, I. A.; Soon, C. P.; Laughton, K. J. *Neurochem.* **2009**, *108*, 1198.
- (17) Paresce, D. M.; Chung, H.; Maxfield, F. R. *J. Biol. Chem.* **1997**, *272*, 29390.
- (18) Nielsen, H. M.; Mulder, S. D.; Beliën, J. A.; Musters, R. J.; Eikelenboom, P.; Veerhuis, R. *Glia* **2010**, *58*, 1235.
- (19) Liu, J.; Wang, W.; Zhang, Q.; Zhang, S.; Yuan, Z. *Biomacromolecules* **2014**, *15*, 931.

- (20) Qiu, Y.; Liu, Y.; Wang, L.; Xu, L.; Bai, R.; Ji, Y.; Wu, X.; Zhao, Y.; Li, Y.; Chen, C. *Biomaterials* **2010**, *31*, 7606.
- (21) Malugin, A.; Ghandehari, H. *J. Appl. Toxicol.* **2010**, *30*, 212.
- (22) Chafekar, S. M.; Malda, H.; Merckx, M.; Meijer, E. W.; Viertl, D.; Lashuel, H. A.; Baas, F.; Scheper, W. *ChemBioChem* **2007**, *8*, 1857.
- (23) Bitan, G.; Kirkitadze, M. D.; Lomakin, A.; Vollers, S. S.; Benedek, G. B.; Teplow, D. B. *Proc. Natl. Acad. Sci. U.S.A.* **2003**, *100*, 330.
- (24) Schmidt, M.; Sachse, C.; Richter, W.; Xu, C.; Fändrich, M.; Grigorieff, N. *Proc. Natl. Acad. Sci. U.S.A.* **2009**, *106*, 19813.
- (25) Sachse, C.; Xu, C.; Wieligmann, K.; Diekmann, S.; Grigorieff, N.; Fändrich, M. *J. Mol. Biol.* **2006**, *362*, 347.
- (26) Schmidt, M.; Sachse, C.; Richter, W.; Xu, C.; Fändrich, M.; Grigorieff, N. *Proc. Natl. Acad. Sci. U.S.A.* **2009**, *106*, 19813.
- (27) Walsh, D. M.; Lomakin, A.; Benedek, G. B.; Condron, M. M.; Teplow, D. B. *J. Biol. Chem.* **1997**, *272*, 22364.
- (28) Urbanc, B.; Betnel, M.; Cruz, L.; Bitan, G.; Teplow, D. *J. Am. Chem. Soc.* **2010**, *132*, 4266.
- (29) Kaye, R.; Head, E.; Thompson, J. L.; McIntire, T. M.; Milton, S. C.; Cotman, C. W.; Glabe, C. G. *Science* **2003**, *300*, 486.
- (30) Liu, L.; Zhang, L.; Niu, L.; Xu, M.; Mao, X.; Yang, Y.; Wang, C. *ACS Nano* **2011**, *5*, 6001.
- (31) Zhang, M.; Mao, X.; Yu, Y.; Wang, C.-X.; Yang, Y.-L.; Wang, C. *Adv. Mater.* **2013**, *25*, 3780.
- (32) Li, M.; Howson, S. E.; Dong, K.; Gao, N.; Ren, J.; Scott, P.; Qu, X. *J. Am. Chem. Soc.* **2014**, *136*, 11655.
- (33) Saido, T.; Leissring, M. A. *Cold Spring Harbor Perspect. Med.* **2012**, a006379.
- (34) Chapman, H. A.; Riese, R. J.; Shi, G.-P. *Ann. Rev. Physiol.* **1997**, *59*, 63.
- (35) Mueller-Stieber, S.; Zhou, Y.; Arai, H.; Roberson, E. D.; Sun, B.; Chen, J.; Wang, X.; Yu, G.; Esposito, L.; Mucke, L. *Neuron* **2006**, *51*, 703.
- (36) Bertini, I.; Gonnelli, L.; Luchinat, C.; Mao, J.; Nesi, A. *J. Am. Chem. Soc.* **2011**, *133*, 16013.
- (37) Yesuvadian, R.; Krishnamoorthy, J.; Ramamoorthy, A.; Bhunia, A. *Biochem. Biophys. Res. Commun.* **2014**, *447*, 590.
- (38) Savelieff, M. G.; Liu, Y.; Senthamarai, R. R.; Korshavn, K. J.; Lee, H. J.; Ramamoorthy, A.; Lim, M. H. *Chem. Commun.* **2014**, *50*, 5301.